Automatic Cardiac 4D Segmentation Using Level Sets

Karl D. Fritscher, Roland Pilgram, and Rainer Schubert

Institute for Biomedical Image Analysis, University for Health Sciences,
Medical Informatics and Technology, Hall in Tirol, Austria
Karl.Fritscher@umit.at

Abstract. For the analysis of shape variations of the heart and the cardiac motion in a clinical environment it is necessary to segment a large amount of data in order to be able to build statistically significant models. Therefore it has been the aim of this project to find and develop methods that allow the creation of a fully automatic segmentation pipeline for the segmentation of endocardium and myocardium in ECG-triggered MRI images. For this purpose a combination of a number of image processing techniques, from the fields of segmentation, modeling and image registration have been used and extended to create a segmentation pipeline that reduces the need for supplementary manual correction of the segmented labels to a minimum.

1 Introduction

The analysis of shape and shape variations of organs and anatomical structures in general has become an important field of medical image processing. Detailed shape analysis gives the possibility to identify typical variations among healthy individuals in order to be able to distinguish them from pathological variations and improve the early diagnosis of diseases, which result in pathological variations of shape. Since the heart is a dynamic organ, not only the analysis of the cardiac shape, but also the analysis of the cardiac motion is a major topic in medical image analysis. For this purpose, the heart has to be segmented not only at one particular time, but during one cardiac cycle, which is typically consisting of 15-20 images using ECG-triggered MRI images. Due to the fact that such large amounts of data are needed in order to perform analysis of shape and shape variations, it has been the objective of this project to develop a pipeline that is providing methods, which allow fully automated and at the same time robust and effective segmentation of cardiac MRI-images.

In the last decade, deformable models [1] emerged as a well established method for medical image segmentation. Beside of parametric deformable models [1] also known as “snakes”, introduced by Kass and Terzopoulos, geometric deformable models based on level sets [2, 3] became one of the most used methods in medical segmentation pipelines. The fact, that geometric deformable models can easily handle topological changes and are easily expandable from two to three dimensions made them a frequent choice for a number of extensions to the geometric deformable models originally introduced by Sethian and Osher [2, 3].

One characteristic of deformable models is that the segmentation process has to be started by providing an initial surface, which will be deformed and adapted to the

A.F. Frangi et al. (Eds.): FIMH 2005, LNCS 3504, pp. 113 – 122, 2005.

image data by minimizing an energy functional. One possibility to generate such an initial surface, which is ideally already a good approximation of the structure to be segmented is to use user defined seed points and take them as a basis for e.g. fast marching segmentation [4]. The disadvantage of using these methods is, that they need user interaction to set the seed points and the resulting initial surface is very dependent on the location of the seed points. Therefore a better solution is to use a pre-defined initial surface to start the level set segmentation. One possibility to fulfill this task is to create a common shape template the from a number of segmented data sets by using principal component analysis [5]. The term common shape template is used, since we are only using the mean shape for initialization and not to guide the segmentation process, where the whole common shape model – including the principal components – would be used.

Having an initial surface, this surface has to be positioned - ideally - as near as possible to the boundaries of the structure to be segmented. For this purpose a registration of the dataset to be segmented, with the common shape template has to be performed. This can be done by registering the individual dataset and an atlas, containing the common shape template and a grayscale image that has once been aligned to the common shape template. A good choice for performing this task is to use mutual information metric [6].

For the segmentation of the whole cardiac cycle the segmented label from one point in time of the cardiac cycle can be used as initial template for the next point in time. The initial template for the myocardium segmentation is generated by creating distance maps of the segmented endocardium to produce initial templates for the myocardium. The final myocardium segmentation is again performed using level set segmentation.

Summing up, the objective of this project was to generate a pipeline for automatic segmentation of the endocardium and myocardium for a whole cardiac cycle, by using a common shape template for the initialization of the segmentation. For this purpose two main tasks had to be fulfilled

1. Building a common shape template of the four chambers of the heart in order to initialize the segmentation process.
2. Generating a segmentation pipeline that uses this template for initialization and succeeds in automatically generating labels of the cardiac endocardium and myocardium, which need no or minimal manual correction.

2 Methods

2.1 Geodesic Snakes/Geometric Deformable Models

Although parametric deformable models are quite intuitive to implement, they are also having some weaknesses, which are partially limiting the usability of this type of models: Firstly, realizing topologically adaptive parametric models, means to do some major modifications of the parametric deformable models, since any change in topology need new parameterization. During the evolution of a contour in the segmentation process, interfaces may change connectivity and split, thereby undergoing a topological transformation which is often very difficult to follow using

traditional approaches. Moreover adapting parametric models to 3 or 4 dimensions is a very challenging task and requires computationally expensive methods [7].

In order to overcome these problems, geometric deformable models have been introduced in the field of image analysis by Caselles and Malladi [8, 9]. They are based on curve evolution theory and level set methods [4].

Being more independent from initialization than parametric deformable models, level sets are also designed to handle problems in which the evolving interfaces can develop sharp corners and cusps and change topology. Hence in order to provide a method, which is on the one hand capable of handling topological changes and on the other hand allow the usage of statistical shape models to guide the segmentation process in the future, geometric deformable models have been preferred to parametric deformable models in the course of this project.

In this project geometric deformable models have been used in two different concepts: Boundary driven geometric deformable models for the endocardium segmentation and region-competition snakes for myocardium segmentation.

Boundary-Driven Geometric Deformable Models. As posted in [10], geometric deformable models are defined as the zero level set of an implicit function ϕ, defined on the entire image. The evolution of the surface is defined via partial differential equation on the implicit function ϕ. Following the approach used by Caselles et al. [9] we are using the following formula

$$\frac{\delta\phi}{\delta t} = c(x)(\kappa + V_0)\left|\nabla(\phi)\right| + \beta(\nabla(P)\cdot\nabla(\phi)) . \tag{1}$$

$\beta(\nabla(P)\cdot\nabla(\phi))$ is the projection of an attractive force vector to the surface. P is the gradient of a potential field, given as

$$P(x, y, z) = \left|(\nabla(G_\sigma * I(x, y, z)))\right| . \tag{2}$$

β denotes the strength of the attractive force and κ is the curvature dependent speed. $c(x)$ is the stopping term based on the image gradient and V_0 is a constant.

The curvature dependent stopping term adds some robustness concerning leakage through object boundaries and prevents the evolving contour from leaking through small gaps.

Region-Competition Snakes. In contrast to boundary driven snakes, geometric deformable models can also be governed by local probabilities that determine if the snake is inside or outside of the structure to be segmented. In this implementation of geometric deformable models, the propagation term is controlled in a way, that it shrinks, when the boundary encloses parts of the background and grows, when the boundary is inside the wanted regions [11].

In our implementation, based on the itkTresholdSegmentationLevelSetImageFilter of the Insight Segmentation and Registration Toolkit (ITK) [12] a speed term (feature image) with positive values inside an intensity window (between a low and high threshold) and negative values outside that intensity window is constructed. The evolving level set front will lock onto regions that are at the edges of the intensity

window. In detail the feature image is calculated as follows (L…lower threshold, U…upper threshold).

$$f(x) = \begin{cases} g(x) - L & if\ g(x) < (U-L)/2 + L \\ U - g(x) & otherwise \end{cases} . \tag{3}$$

In our application the thresholds can be calculated by calculating the mean grey value and standard deviation of the pixels, which are at the position of the template image in the original grayscale image. The thresholds are set by taking the mean grey value of the template region ± 1 standard deviation.

Furthermore, a Laplacian calculation on the image to the threshold-based speed term can be added. The Laplacian term causes the evolving surface to be more strongly attracted to image edges.
Identically to boundary driven snakes, an additional curvature based smoothing term adds robustness concerning leakage through object boundaries.

2.2 Model Building

Signed Distance Maps. For the purpose of building models of already segmented label data, we were choosing distance maps as a representation of shape following the approach of Leventon et al. [5]. A curve *C* which should be represented is embedded as the zero level set of a higher dimensional surface u, whose height is sampled at regular intervals. Each sample encodes the distance to the nearest point on the curve, with negative values inside the curve. The unsigned surface *u* is defined as

$$|u(x)| = \min_q \|C(q) - x\| . \tag{4}$$

Distance maps have the property, that the gradient magnitude of the image is constant across the image and equal to one. The direction of the gradient is equal to the outward normal of the nearest point on the curve C. From any point x in space the nearest point on the curve can be computed by

$$x - u(x)\nabla u(x) . \tag{5}$$

A distance map provides the propagation of the boundary information without loss of fidelity and the redundancy of information over a region in space provides stability in many types of computation.

Alignment of Distance Maps. In order to rigidly align the distance map representations of the individual labels, we were using mutual information (MI) independently introduced by Viola and Wells [6].

Given two variables U and V, mutual information is defined as

$$MI(U,V) = H(U)+H(V)-H(U,V). \tag{6}$$

Already applied to a wide range of applications for multi modality registration, MI turned out to be also very useful for the global alignment of distance functions and provided very reasonable results for the alignment of our signed distance maps.

Principal Component Analysis on Signed Distance Maps. Having a training set of signed distance maps, Principal Component Analysis can be used to derive a shape model [13]. A mean surface can be computed by taking the mean of the signed distance functions. The matrix of eigen-vectors and the diagonal matrix of corresponding eigen-values is computed from the co-variance matrix using Single Value Decomposition.

An estimate of a novel shape, u, can be represented by k principal components in a k-dimensional vector of coefficients, α:

$$\alpha = U_k^T (u - \mu) . \tag{7}$$

U_k is a matrix consisting of the first k columns of the matrix of eigen-vectors U, which is used to project a surface into the eigen-space. Given the coefficients α, an estimate of the shape u is reconstructed from U_k and μ :

$$\tilde{u} = U_k \alpha + \mu . \tag{8}$$

Since distance transforms do not form a linear vector space, $\tilde{u}$ will in general not be a true distance function. However, the surfaces still have the properties of smoothness and local dependence, which is sufficient for our purposes [5].

2.3 Model to Image Registration

In order to register the common shape template to a new image, we are also using mutual information by rigidly aligning the grey-scale image, on whose segmented label data all other label data sets have been registered, and the image to be segmented.

For this purpose a multi-resolution registration approach has been used. This means that the images are registered in an iterative process, using different resolutions of the images. This fact adds robustness to the registration process and increases speed and accuracy.

3 Results

In the course of this project, we have been developing a C++ software-pipeline for fully automatic segmentation of 4D heart MRI datasets. This pipeline is implementing the methods described above, by using and extending some of the functionality of the Insight Segmentation and Registration Toolkit (ITK) and the Visualization Toolkit (VTK) [14].

As a first step we had to create a common shape template out of 10 segmented heart datasets. Since we also wanted to have the possibility to segment the four chambers of the heart separately, we have not only been creating a common shape template of the whole endocardium, but also of each chamber of the heart. For this purpose we created distance maps of the datasets, and rigidly aligned them by using mutual information. Fig. 2 is showing the results of the registration of the whole endocardium and of the left ventricle each with 5 datasets.

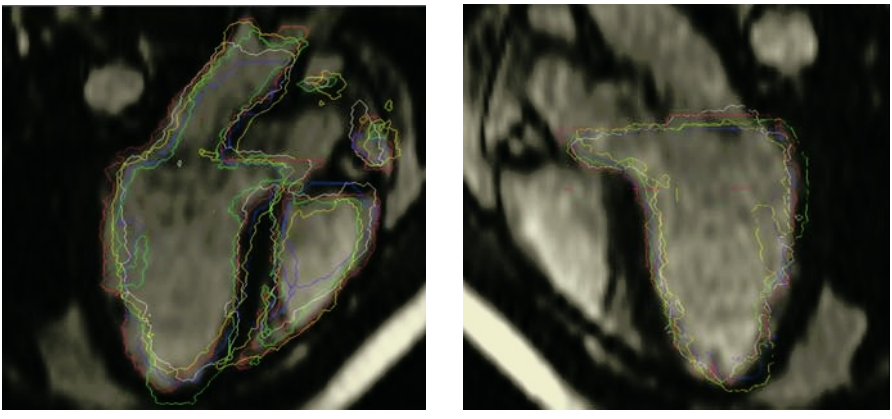

Fig. 1. Result of the rigid alignment of 5 labeled heart datasets. Left: Registered endocardium, Right: Registered left ventricles

Of course rigid alignment does not provide perfect correspondence, however, for the task of building a model/template to initialize the segmentation process and using signed distance maps, which are robust to slight misalignment as a representation of shape, we did not necessarily need perfect correspondence.

Using the methods described in section 2.2 we were calculating the common shape template and its principal components. Note, that the main variations of the model represented by the principal components are not involved in the segmentation process up to now, however, this might be part of our future work. Moreover, at this point of time the principal components are an additional important criterion to evaluate the validity of the model for our purposes. Fig. 2 is showing the common shape templates of the 4 chambers of the heart.

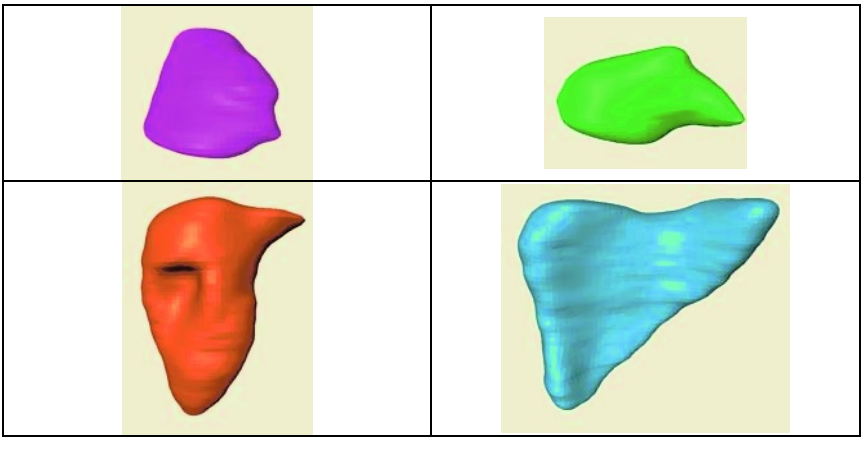

Fig. 2. Common shape templates of the four heart chambers. Top row: left atrium (left), right atrium (right), bottom row: left ventricle (left), right ventricle (right)

Having these initial templates the image to be segmented has been registered to the grayscale image containing the label data on which the distance maps have been registered, using mutual information. Another possibility would have been to directly register the new image to the distance map of the common shape template, however, in this case, the results turned out to be less robust and less correct, than in the first case.

The active geodesic level set segmentation process itself is started by using the common shape templates as initial templates and setting predefined parameters for the level set algorithm. As stopping criteria a threshold for the amount of change of the zero level set between two segmentation iterations has been used. Additionally a maximum number of iterations has been set. Due to the fact, that the segmentation is initialized very near to the object boundaries, the propagation scaling (~balloon force) can be set rather low. This brings the advantage that leaking through boundaries is less likely and the geometric deformable model is guided by the advection force, pulling the contour to edges in the image and the curvature term, preventing the contour from leaking and resulting in more robust convergence.

Fig. 3 is showing the initial templates and the results of endocardium segmentation. Note that the borders between atria and ventricles have not been manually corrected.

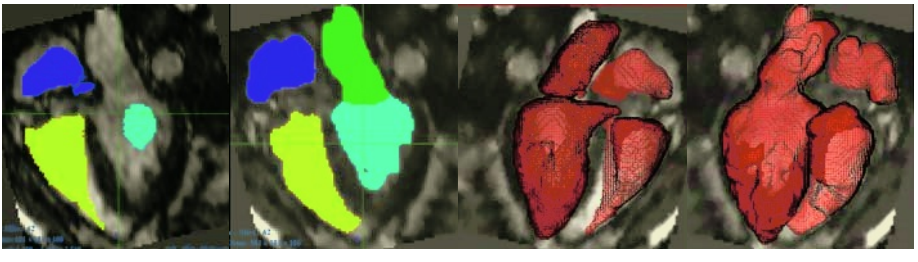

Fig. 3. Endocardium segmentation. Comparison of initial state and segmentation result of a endocardium segmentation in 2D (first two images) and 3D (third and fourth image)

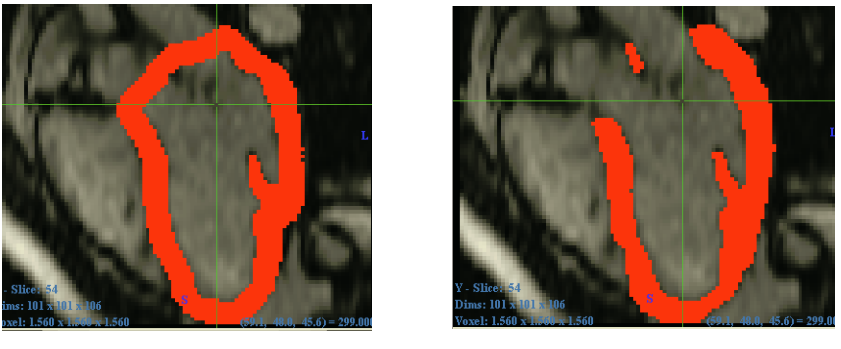

Fig. 4. Example for a template of the myocardium segmentation of the left ventricle generated via distance maps (left) and the final segmentation result for the left ventricle myocardium (right)

For the segmentation of the cardiac cycle, the segmentation results of the initial point in time have been used as initial templates [15]. For this purpose, the same transformation as for the first image has to be applied to the whole dataset of the cardiac cycle. An initial template for the myocardium segmentation can be generated by thresholding a signed distance map of the endocardium labels, for each chamber. Using this as an initial template, the thresholds for the region-competition snakes are computed by calculating the mean grey value of the pixels covered by the label. The thresholds are set by adding ±1 standard deviation to this mean value.

In this work the correctness of the segmentation has been evaluated for two different heart datasets: One dataset of the ten datasets, which have been used for the model building process (1) and one new dataset (2). In order to evaluate the correctness of the segmentation for the datasets, the generated labels have been compared with the labels after manual correction of the segmentation results, considering this as the gold standard. For endocardium and myocardium segmentation a similarity index for three different points in time of the cardiac cycle has been calculated by using

$$S = \frac{2|A \cap B|}{|A| + |B|}. \tag{9}$$

A and B are the non-zero pixels in the first and second input images. Operator $|\bullet|$ represents the size of a set and $\cap$ represents the intersection of two sets.
Table 1 is showing the results for the similarity indexes:

Table 2 is showing the undirected Hausdorff distances, comparing the automatically segmented endocardium and the manually corrected labels.

Table 1. Similarity indexes for automatic segmentation results and manually corrected segmentation results for two heart data sets (0, 60 and 110 ms after the R-peak in the ECG)

Similarity index	000 ms		060 ms		110 ms	
	Heart 1	Heart 2	Heart 1	Heart 2	Heart 1	Heart 2
Endocardium	0.980	0.992	0.970	0.980	0.971	0.976
Left ventricle	0.991	0.991	0.998	0.992	0.998	0.976
Right Ventricle	0.946	0.988	0.933	0.976	0.927	0.918
Left atrium	0.975	0.984	0.988	0.976	0.979	0.930
Right atrium	0.986	0.990	0.989	0.961	0.948	0.953
Myocardium	0.950	0.964	0.952	0.958	0.940	0.936

Table 2. Hausdorff distances in mm between automatic segmentation results and manually corrected segmentation results for two heart data sets (0, 60 and 110 ms after the R-peak in the ECG)

Hausdorff distance	000 ms		060 ms		110 ms	
	Heart 1	Heart 2	Heart 1	Heart 2	Heart 1	Heart 2
Endocardium	2.3	2.0	2.7	2.5	2.7	2.5
Myocardium	5.1	4.8	5.3	5.2	5.8	6.1

4 Discussion

Using mutual information to register the distance maps of the individual labels and the grayscale images to the atlas resulted in a precise rigid alignment and provided very satisfying results. Calculating a mean model resulted in a meaningful and feasible common shape template, which proved to be an adequate tool for the initialization of the level set segmentation process. Using geodesic level sets for the segmentation of the endocardium turned out to be an adequate choice and resulted in good segmentation results compared to the gold standard. Note that no manual correction has been performed between the segmentation of the different phases of the cardiac cycle. Performing minimal manual correction - especially the correction of the valve plane level - after segmenting the first point in time of the cardiac cycle would of course mean another improvement of the segmentation results.

The usage of ITK and VTK to implement the segmentation pipeline turned out to be an adequate choice for programming the software pipeline.

A detailed and comprehensive evaluation of the presented pipeline and an extension of the pipeline, which is using a modified template created out of more datasets and using other forms of shape representation in order to implement knowledge about shape variations in the segmentation process itself is currently under development.

Acknowledgement

We would like to thank the Department of Cardiology, Head: Univ. Prof. Dr. O. Pachinger and the Department of Radiology I, Head: Univ. Prof. Dr. W. Jaschke of the University Clinic Innsbruck for the acquisition of the MRI data. This project has been supported by the “Forschungsförderungsfonds für die gewerbliche Wirtschaft” (FFF- Austria).

References

[1] M. Kass, A. Witkin, D. Terzopoulos, "Snakes: active contour models", *International Journal on Computer Vision*, vol. 1, pp. 321-331, 1987.

[2] Sethian, J. A., "Curvature and evolution of fronts", *Commun. Math. Phys.*, vol. 101, 1985.

[3] J. Osher, J. A. Sethian, "Fronts propagating with curvature-dependent speed: algorithms based on Hamilton-Jacobi formulations", *Journal of Computational Physics*, vol. 79, pp. 12-49, 1988.

[4] Sethian, J. A., "Level Set Methods and Fast Marching Methods: Evolving Interfaces in Computational Geometry, Fluid Mechanics, Computer Vision and Material Science", 2nd Edition ed, Cambridge University Press, 1999.

[5] Leventon, M., "Statistical Models for Medical Image Analysis", in *Artificial Intelligence Lab.*: MIT, 2000.

[6] P. Viola, W M. Wells, "Alignment of maximization of mutual information", *International Journal on Computer Vision*, vol. 22, pp. 61-97, 1997.

[7] T. McInerney, D. Terzopoulos, "T-snakes: Topology adaptive snakes", *Medical Image Analysis*, vol. 4, pp. 73-91, 2000.
[8] R. Malladi, J. A. Sethian, B. C. Vemuri, "Shape modeling with front propagation: a level set approach", *IEEE TPAMI*, vol. 17, pp. 158-175, 1995.
[9] V. Caselles, R. Kimmel, G. Sapiro, "A geometric model for active contours", *Numerische Mathematik*, vol. 66, 1993.
[10] R. Goldenberg, R. Kimmel, R. Rivlin, E. Rudzsky, "Fast Geodesic Active Contours", *IEEE Transactions Imag. Proc.*, vol. 10, pp. 1476-1475, 2001.
[11] S. C. Zhu, A. Yuille, "Region Competition: Unifying Snakes, Region Growing, and Bayes/MDL for Multiband Image Segmentation", *IEEE Transactions on Pattern Analysis and machine Intelligence*, vol. 18, 1996.
[12] http://www.itk.org.
[13] M. Leventon, E. Grimson, O. Faugeras, "Statistical Shape Influence in Geodesic Active Contours", *Computer Vision and Pattern Recognition*, vol. 1, pp. 316-323, 2000.
[14] http://www.vtk.org.
[15] K. D. Fritscher, R. Schubert, "A software framework for pre-processing and level set segmentation of medical image data" presented at SPIE Medical Imaging, San Diego, 2005.